Full Paper

A Penicillamine Biosensor Based on Tyrosinase Immobilized on Nano-Au/ PAMAM Dendrimer Modified Gold Electrode

Nian Bing Li,[a,b] *Juhyoun Kwak*[a]*

[a] Department of Chemistry, Korea Advanced Institute of Science and Technology (KAIST), Daejeon, Korea
[b] School of Chemistry and Chemical Engineering, Southwest University, Chongqing 400715, P. R. China
*e-mail: jhkwak@kaist.ac.kr

Received: June 11, 2007
Accepted: July 11, 2007

Abstract
Gold electrodes were modified with submonolayers of 3-mercaptopropionic acid and further reacted with poly(amidoamine) (PAMAM) dendrimers to obtain thin films. The high affinity of PAMAM dendrimer for nano-Au with its amine groups was used to realize the role of nano-Au as an intermediator to immobilize the enzyme of tyrosinase. The characterization of the modified electrode was investigated by cyclic voltammetry, electrochemical impedance spectroscopy and atomic force microscopy (AFM). Tyrosinase can catalyze the oxidation of catechol to *o*-benzoquinone. When penicillamine was added to the solution, it reacted with *o*-benzoquinone to form the corresponding thioquinone derivatives, which resulted in decrease of the reduction current of *o*-benzoquinone. Based on this, a new electrochemical sensor for determination of penicillamine has been developed.

Keywords: Penicillamine, Tyrosinase, Nano-Au, PAMAM, Catechol, Biosensor

DOI: 10.1002/elan.200703968

1. Introduction

Penicillamine (PCA) is a sulfhydril amino acid with a hydrogen ion in the beta-carbon of cysteine replaced by the methyl group. In addition to chelation of heavy metals, such as copper, it suppresses the cross-linking of collagen by formation of a thiazolidine bond with the aldehyde group of collagen [1]. It is particularly efficacious in extra-articular complications, such as vasculitis, amyloidosis, and pulmonary manifestations [2]. PCA is a medication, used for many years in the treatment of various rheumatic diseases, most commonly in rheumatoid arthritis [3]. It is also classified as a metal binding (or chelating) agent used in the treatment of Wilson's disease, a genetic disease that results in excessive copper deposits in the body tissues. Increasing the amount of PCA can cause rashes early in treatment. It can also cause loss of appetite, nausea, abdominal pain, and loss of the sense of taste. PCA can also cause bone marrow suppression and serious kidney disease. All patients who take PCA require regular blood and urine tests for monitoring.

Various methods have been proposed for the determination of PCA including spectrophotometry [4–7], fluorometry [8, 9], chemiluminescence [10, 11], potentiometry [12], high performance liquid chromatography (HPLC) [13–15], capillary electrophoresis [16, 17] and NMR spectroscopy [18]. Electrochemical methods are an alternative for the PCA determination because they are cheap, simple, fast and sensitive [19–22]. Saeed Shahrokhian et al. reported that the cobalt salophen (CoSal)-modified carbon-paste electrode showed an excellent electrocatalytic effect toward the oxidation of PCA. Based on the voltammetric studies of electrooxidation of PCA, an electrochemical sensor for the determination of PCA has been fabricated [19]. Orawon Chailapakul et al. used the boron-doped diamond thin film electrode to study PCA by using cyclic voltammetry. Hydrodynamic voltammetry and flow injection analysis with amperometric detection were used to determine PCA [20]. Torriero et al. immobilized the tyrosinase on 3-aminopropyl-modified controlled-pore glass to form a microrotating disk bioreactor. A sensitive method for determination of PCA has been verified by on-line interfacing of a rotating biosensor and continuous low/stopped-flow operation [21]. Saeed Shahrokhian et al. also studied the electrochemical behavior of dopamine in the presence of PCA at the surface of glassy carbon electrode. The electrochemically initiated reaction of dopaminoquinone with PCA was used to provide an appropriate electroanalytical signal, which can be related to the PCA concentration [22].

Poly(amidoamine) (PAMAM) dendrimers have attracted increasing attention in recent years because of their unique structure, interesting properties, as well as their potential applications in medicine, catalysis, gene therapy, and nanoreactor systems [23–25]. PAMAM dendrimers are monodisperse, highly branched polyelectrolytes with ammonium functional groups on the surface (primary amine) and at the branch points in the interior (tertiary amine). Although most of the work with dendrimers has been carried out in solution, these compounds have also been used to modify electrode surfaces and some recent reports indicate that these materials are capable of increasing the concentration

of hydrophobic molecules at the electrode – solution interface, improving in this way the sensitivity as well as the selectivity of certain specific electrochemical reactions [26 – 28].

In recent years, the use of gold nanoparticles (nano-Au) is attracting more interest for the preparation of biosensors [29]. Nano-Au can provide a stable surface for enzyme immobilization, and allow the electrochemical sensing to be performed without the need of any other electron mediators. Moreover, the conductivity properties of nano-Au allow us to design simple, sensitive and stable electroanalytical procedures based on enzyme immobilization [30, 31].

In the present work, we have focused on the study of the suitability of the tyrosinase / nano-Au particles/ PAMAM dendrimers modified electrode for the development of the PCA biosensor using self-assembly technique. Tyrosinase is a type (III) copper protein and is widely distributed in microorganisms, plants and animals [32]. Tyrosinase can catalyze the oxidation of *o*-diphenols to *o*-quinones whose electrochemical reduction peak appeared at about the potential of 20 mV. If, however, there are trace amounts of PCA, owing to PCA as a nucleophilic agent, which easily reacts with *o*-quinone to produce a new compound through the Michael Addition reactions, the reduction peak current decreased. Based on this phenomenon, a new biosensor for determination of PCA was developed.

2. Experimental

2.1. Reagents

Amine terminated G4 poly(amidoamine) dendrimer (PAMAM), 3-mercaptopropionic acid (MA), and catechol were purchased from Aldrich. *N*-(3-dimethylaminopropyl)-*N*′-ethylcarbodiimide hydrochloride (EDC), gold colloid and the enzyme tyrosinase (from mushroom, EC 1.14.18.1, 2130 U mg^{-1}) was obtained from Sigma. PCA was purchased from Alfa Aesar. Phosphate buffer solution (PBS) with various pH values were prepared by mixing the stock solutions of NaH_2PO_4 and Na_2HPO_4. All chemicals used were of analytical-reagent grade, and water (> 18 MΩ cm) was obtained from a Millipore Milli-Q purification system.

2.2. Apparatus

The cyclic voltammetry (CV), square-wave voltammetry and electrochemical impedance measurements were performed with an Autolab potentiostat 10 (Ecochemie). A three-electrode system used in the measurements consists of a gold electrode or a modified gold electrode as the working electrode, platinum wire as the counter electrode, and a Ag/AgCl electrode as the reference electrode. All potentials are given with respect to the Ag/AgCl electrode. Atomic force microscopy (AFM) imaging was performed in the Tapping Mode on a Nanoscope IIIa multimode scanning probe microscope (Veeco, USA) with Tapping Mode etched silicon probes (TESP).

2.3. Electrode Preparation

Scheme 1 describes the basic strategy for the preparation of tyrosinase modified electrode. Gold electrodes were prepared by electron beam evaporation of 40 nm of Ti followed by 150 nm of Au onto Si (100) wafers. The electrode was cleaned in piranha solution (30% H_2O_2/70% H_2SO_4), rinsed with water, and then dried with nitrogen gas. (WARNING:

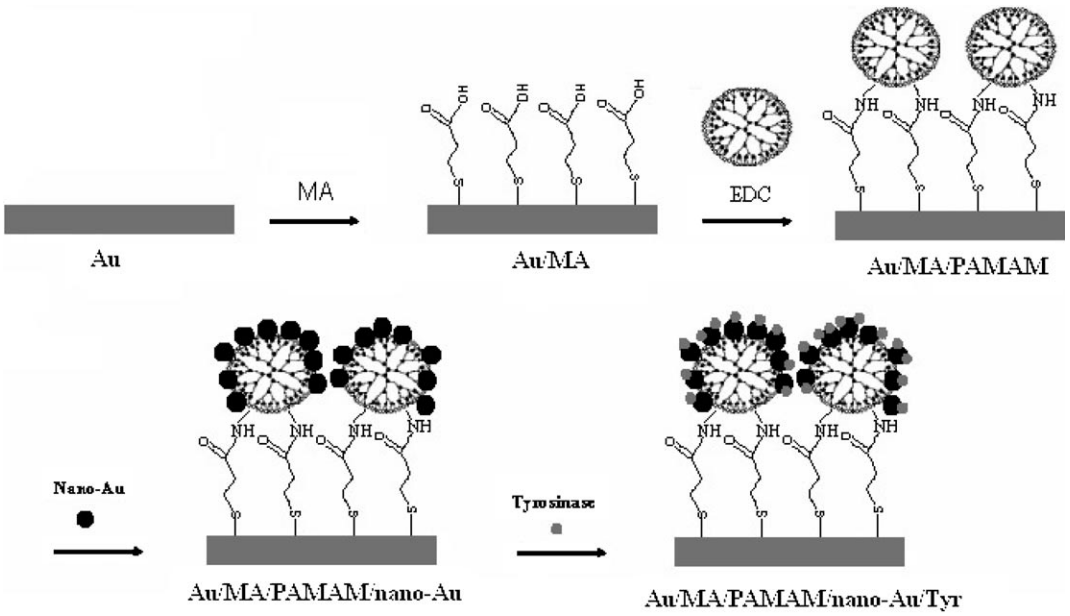

Scheme 1. Schematic representation of the surface modification process and fabrication of a tyrosinase biosensor

piranha reacts violently with organics). The pretreated electrode was immersed in 1.0 mol L^{-1} ethanol solution of MA (75/25% ethanol/water) for 12 h at room temperature and then washed thoroughly in 75/25% ethanol/water to remove the nonchemisorbed materials. Subsequently, the Au/MA modified electrode was immersed in 1.0 mg mL^{-1} PAMAM dendrimer solution in presence of 5 mmol L^{-1} EDC for 12 h period at room temperature. Under these conditions, EDC [33], a well-known coupling activation agent, was assumed to promote the formation of peptide bonds. Thus surface anchoring of dendrimers G4 PAMAM on the thiol modified gold electrodes was carried out by means of peptidic bond formation using traditional peptide chemistry protocols. After rinsed with distilled water, the Au/MA/PAMAM membrane electrode was transferred into gold colloid solution for 12 h at 4 °C. Then the nano-Au modified electrode (Au/MA/PAMAM/nano-Au) was incubated in 5 mg mL^{-1} tyrosinase (Tyr) for 12 h and the Au/MA/PAMAM/nano-Au/Tyr modified electrode was fabricated.

3. Results and Discussion

3.1. Electrochemical Characteristics of the Tyrosinase Modified Electrode

The surface morphology of each step of the electrode modification process was shown in Figure 1 by atomic force microscope (AFM). Figure 1a shows an image of MA film self-assembled on a bare gold electrode surface. Although the fraction of the electrode surface chemically modified is far less than unity, previous studies suggest that the thiol molecules in this submonolayer are not forming islands or clusters but instead are individually distributed across the electrode surface. Figure 1b presents the AFM image of PAMAM dendrimers, which anchored on the surface of MA monolayer. It indicates that dendrimer PAMAM molecules tend to form a densely packed film on MA surface in order to maintain lower surface tension. However, it is very difficult to image individual molecules of the dendrimer PAMAM. The AFM image in Figure 1c of nano-Au anchored on the surface of PAMAM film shows gold

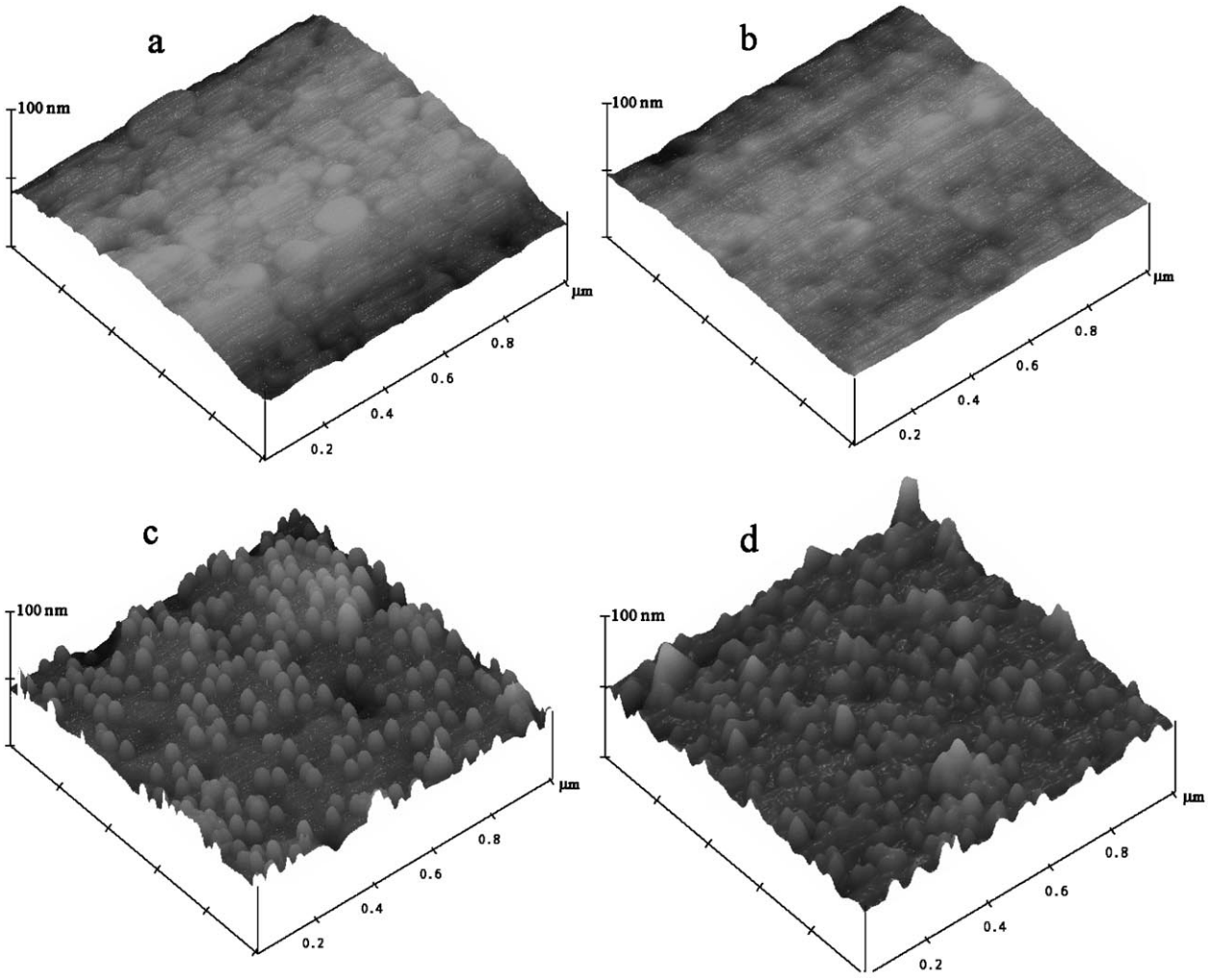

Fig. 1. AFM images of Au/MA electrode (a), Au/MA/PAMAM electrode (b), Au/MA/PAMAM/nano-Au electrode (c), and Au/MA/PAMAM/nano-Au/Tyr electrode (d).

nanoparticles are obviously formed on the PAMAM film. The size of the gold nanoparticles layer is about 20 nm. When the tyrosinase was immobilized on the nano-Au surface, the AFM image (Fig. 1d) indicates that the enzyme film is even more uniform and smooth that that of nano-Au film.

Cyclic voltammetry is an effective method for probing the feature of surface-modified electrode and testing the kinetic barrier of the interface because the electron transfer between solution species and the electrode must occur by tunneling either through the barrier or through the defects in the barrier. Therefore, CV was chosen as a marker to investigate the changes of electrode behavior after each assembly step. Figure 2A shows the results of the CVs of the bare gold electrode and different modified electrodes during the self-assembled process in the presence of redox probe, $Fe(CN)_6^{4-/3-}$, measured at the appropriate potential window. Focusing on the shape of the responsive curves, it is clear that, the voltammetric curves for the $Fe(CN)_6^{3-}$ anion show a typical reversible shape at the bare gold electrode (Fig. 2Aa). It was concluded that MA molecule self-assembled on Au electrode charged negatively at our experimental condition [34], so the corresponding voltammetric response on the MA modified electrode (Fig. 2Ab) is characterized by a distorted shape and a decrease in the CV current that suggests an impeditive electron transfer behavior. When the PAMAM compounds are further incorporated on the Au/MA electrode surface, the peak currents of probe $Fe(CN)_6^{3-}$ ion on the Au/MA/PAMAM electrode (Fig. 2Ac) increased obviously as compared to those obtained with the MA modified Au electrodes (Fig. 2Ab), this also reflect the electrostatic adsorption between the positively charged surface confined PAMAM molecule under such pH conditions [34], and the negatively charged $Fe(CN)_6^{3-}$ probe. The results show that dendrimer PAMAM G4 was successfully attached to the MA modified gold electrode surfaces, and the Au/MA/PAMAM electrode has a good electrochemical response in $K_3Fe(CN)_6$ solution. To further verify that peptidic bond formation between the dendrimer G4 PAMAM and MA molecules actually takes place, control experiments were performed in which the PAMAM modified electrode were prepared as previously described but without adding the coupling agent EDC. Under these conditions, electrostatic adsorption of the PAMAM species also takes place; CV responses also rise similar to those presented in the presence of EDC. However, when the electrodes are rinsed, and immersed in pure supporting electrolyte solution under stirring conditions, the PAMAM compounds are released from the electrode surface, as evidenced by the decreased CV response that is obtained when the electrodes are later introduced in $Fe(CN)_6^{3-}$ solutions. On the other hand, after the rinsing process just described, the CV response of $Fe(CN)_6^{3-}$ is fully retained for PAMAM-modified electrode in the presence of EDC, so peptidic bond formation takes place between the PAMAM dendrimer molecules and the surface attached MA species. Comparison of Figure 2Ac, Fig. 2Ad showed that the peak currents slightly increased after nano-Au modification. The reason is that nanometer-sized gold colloids play an important role similar to a conducting wire or electron-conducting tunnel, which makes it easier for the electrons transfer to take place. So we can know that the nano-Au was modified on the gold electrode. However, the peak current decreased (Fig. 2Ae) and the potential separation between the cathodic and anodic peaks of the redox probe increased after the tyrosinase was immobilized on the electrode, which indicated that the immobilization of enzyme insulated the electrode and perturbed the interfacial electron transfer considerably.

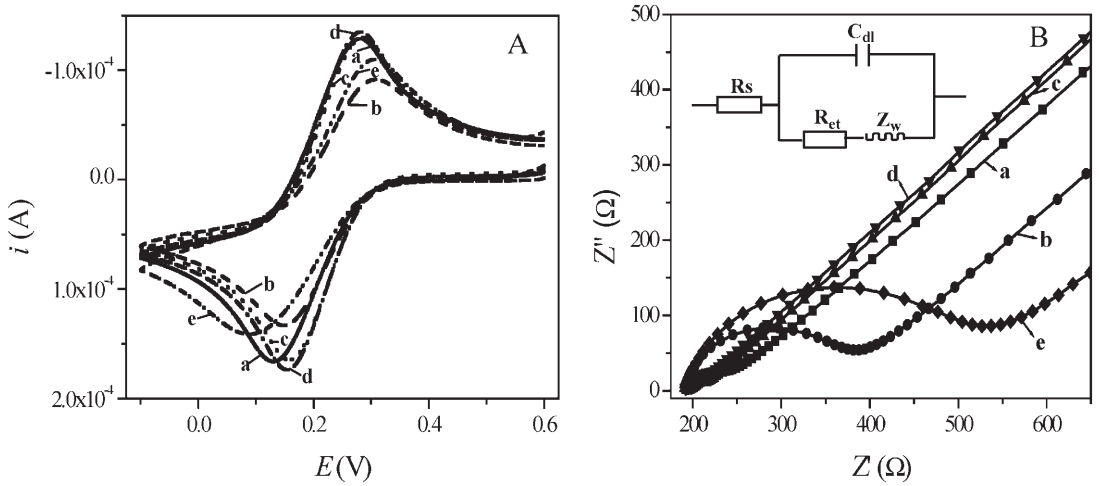

Fig. 2. Cycle voltammograms (A) and the complex impedance plots (B) of different electrodes in the solution of 2.5 mmol L^{-1} $K_3Fe(CN)_6$ + 0.125 mol L^{-1} KCl + 0.05 mol L^{-1} PBS (pH 7.4). Scan rate, 100 mV s^{-1}. The frequency range is at $0.05 - 10^5$ Hz at the formal potential of 0.22 V (vs. Ag/AgCl). a) Bare Au electrode, b) Au/MA electrode, c) Au/MA/PAMAM electrode, d) Au/MA/PAMAM/nano-Au electrode, and e) Au/MA/PAMAM/nano-Au/Tyr electrode. Inset was the equivalent circuit model used to fit the impedance data. C_{dl} represents double layer capacitance; R_{et} is the electron transfer resistance; Z_w is the Warburg impedance; R_s represents the resistance of the electrolyte solution.

Electrochemical impedance spectroscopy (EIS) is one of the most powerful electroanalytical techniques frequently used in studying the electron transfer kinetics [35, 36]. Impedance measurements have also been investigated as a highly sensitive approach. Impedance measurements were performed in the frequency range from 0.05 to 10^5 Hz. Complex impedance plots of bare gold electrode (a), Au/MA electrode (b), Au/MA/PAMAM electrode (c), Au/MA/PAMAM/nano-Au electrode (d) and Au/MA/PAMAM/nano-Au/Tyr electrode (e) are shown in Figure 2B. At the same time, the equivalent circuit shown Figure 2B was used to fit the impedance spectroscopy. The electron transfer resistance, R_{et}, was determined and the results are listed in Table 1. The electron transfer resistance of a bare gold electrode is 30 Ω (Fig. 2Ba). It agrees with the fact that the electron transfer process is very fast, which is a diffusional limited electron transfer process. After MA monolayer self-assembled on Au electrode, the interfacial electron-transfer resistance R_{et} corresponding to the respective semicircle diameters increased obviously (164.6 Ω for curve b in Fig. 2B). The nonconductivity characteristic of MA (SH–CH_2–CH_2–COOH) film and a large quantity of negative charges from -COO^- groups perturbed the interfacial electron-transfer rates between the electrode and the electrolyte solution. After modified by PAMAM, the positively charged surface confined PAMAM molecule would attract negative redox marker, thus R_{et} decreased to 17.6 Ω (Fig. 2B curve c), even much lower than bare Au electrode (Fig. 2Ba). After absorption of nano-Au to the electrode surface, it was surprising to find the R_{et} obviously decreased again (Fig. 2B curve d, $R_{et} = 8.2$ Ω), implying that the nano-Au made electron-transferred easier [37]. Subsequently, when the tyrosinase was absorbed on the surface via nano-Au, R_{et} increased obviously (284.9 Ω for curve e in Fig. 2B), it indicated that the tyrosinase was strongly bound to gold nanoparticles and this decreased the ability of nanoparticles transferring electron. On the basis of the EIS results, it was concluded that tyrosinase was successfully immobilized on the modified electrode.

3.2. Electrochemical Behavior of Catechol in Absence and Presence of PCA

Curve a in Figure 3 gives the CV at the Au/MA/PAMAM/nano-Au modified electrode in 0.1 mol L^{-1} PBS (pH 7.0) containing 2.0×10^{-4} mol L^{-1} catechol with a scan rate of 100 mV s^{-1}. A couple of broad peaks were observed and the peak currents were smaller compared with the peak currents of 2.0×10^{-4} mol L^{-1} catechol at the Au/MA/PAMAM/nano-Au/Tyr modified electrode. Figure 3, curve b, shows a CV at the tyrosinase modified electrode in an aqueous solution containing 0.1 mol L^{-1} PBS (pH 7.0) and 1.25×10^{-5} mol L^{-1} PCA for a scan rate of 100 mV s^{-1}. A low background without a detectable signal can be observed under the potential window. Cyclic voltammetry of 2.0×10^{-4} mol L^{-1} solution of catechol containing 0.1 mol L^{-1} PBS (pH 7.0) on the tyrosinase modified electrode, shows a well couple of redox peak which corresponds to the transformation of catechol to *o*-quinone and vice-versa within a quasireversible two-electron process (Fig. 3, curve c). The further research results indicated that the reduction peak observed attributed to the direct reduction of the enzymatically-produced quinone at enzyme electrode surface. The steps of the enzymatic reaction on the tyrosinase modified electrode surface were shown as follows:

$$\text{Catechol} \xrightarrow{\text{Tyrosinase}(O_2)} o\text{–Quinone} \quad (1)$$

o-Quinones can be electrochemically reduced to *o*-diphenols using a low over-potential without any electron transfer mediator via the following equation:

$$o\text{-Quinone} + 2H^+ + 2e^- \rightarrow \text{Catechol} \quad (2)$$

When PCA was added in the solution of catechol, compared with the CV of catechol on the tyrosinase modified electrode (Fig. 3, curve c), the oxidation peak potential slightly shifted to positive direction and the peak current increased with

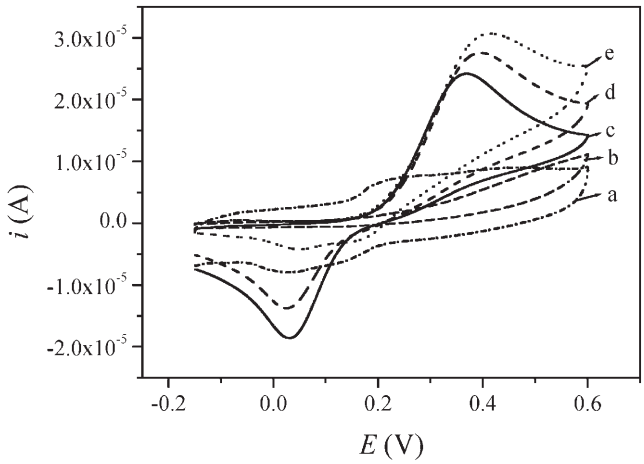

Fig. 3. Cyclic voltammograms of 0.1 mol L^{-1} PBS (pH 7.0) + 2.0×10^{-4} mol L^{-1} catechol at the Au/MA/PAMAM/nano-Au electrode (a); CVs of 0.1 mol L^{-1} PBS (pH 7.0) + 1.25×10^{-4} mol L^{-1} PCA (b); 0.1 mol L^{-1} PBS (pH 7.0) + 2.0×10^{-4} mol L^{-1} catechol (c); 0.1 mol L^{-1} PBS (pH 7.0) + 2.0×10^{-4} mol L^{-1} catechol + 2.5×10^{-5} mol L^{-1} PCA (d); and 0.1 mol L^{-1} PBS (pH 7.0) + 2.0×10^{-4} mol L^{-1} catechol + 5.0×10^{-4} mol L^{-1} PCA (e) at Au/MA/PAMAM/nano-Au/Tyr electrode. Scan rat: 100 mV s^{-1}.

Table 1. Impedance results for the electrodes obtained from Fig. 2B.

No.	Electrode	R_{et} (Ω)
a	Au	30
b	Au/MA	164.6
c	Au/MA/PAMAM	17.6
d	Au/MA/PAMAM/nano-Au	8.2
e	Au/MA/PAMAM/nano-Au/Tyr	284.9

increasing PCA concentration. However, the reduction peak potential did not change with the concentration of PCA increase and the peak current decreased with increase of PCA concentration (Fig. 3, curve d and e). It can be seen that the reduction peak almost disappeared when the concentration of PCA was 5.0×10^{-4} mol L^{-1}. As we known, PCA, which contains sulfhydryl (– SH) and amines (– NH_2) groups, can be as a nucleophile. Under our experimental condition, PCA as a nucleophile reacted with *o*-quinone. Although PCA contain sulfhydryl (– SH) and amines (– NH_2) groups, however, compounds with sulfhydryl groups appear to be far more reactive towards *o*-quinone than amines [38]. For this reason, in the case of the reaction between PCA and *o*-quinone, only the thioether (S-adduct) is formed but no *N*-adduct was observed [39]. The reaction between PCA and *o*-quinone shown in Scheme 2:

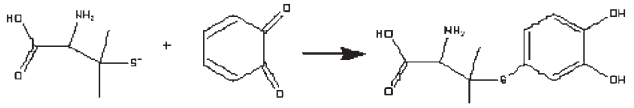

Scheme 2.

According to the fact that the reduction peak potential did not change with the concentration of PCA increase and the square-wave voltammetry (SWV) has more sensitive than cyclic voltammetry, SWV was used to detect the concentration of PCA. The SWVs of different condition are show in Figure 4. Furthermore, the consequent decrease on the height of the *o*-quinone reduction peak can be ascribed to the fact that increasing concentration of PA scavenges the oxidized form of catechol leaving little available for electroreduction. Therefore, the measuring principle of this biosensor for determination of PCA can be described as follows. First, the tyrosinase immobilized on the nano-Au converts catechol to *o*-quinone, and then the quinones are reduced back to catechol at the electrode surface. Second, the detection of the PCA is accomplished by scavenging the oxidized form of catechol and suppressing the substrate recycling process between tyrosinase and the electrode.

3.3. Effect of Different Redox Cosubstrates on the Response of the Biosensor

Other catechol derivatives such as phenol and m-cresol were examined as redox indicators and the results are shown in Figure 5, which shows that the effects of the three redox cosubstrates on the Δi ($\Delta i = i_{\text{catechol derivative}} - i_{\text{catechol derivative–PCA}}$) are different. As can been seen from Figure 5, catechol shows greater sensibility and therefore is selected for this work.

3.4. Effect of pH

The effects of pH on the reduction peak current of 2.0×10^{-4} mol L^{-1} catechol (blank) and 2.0×10^{-4} mol L^{-1} catechol $+2.5 \times 10^{-5}$ mol L^{-1} PCA (sample) between 5.8 and 7.9 in 0.1 mol L^{-1} PBS were studied with SWV technology. As shown in Figure 6, the current response for both blank and sample arrived at a maximum value at pH 7.4. A quantitative evaluation of the change peak current Δi ($\Delta i = i_{\text{catechol}} - i_{\text{catechol–PCA}}$) on the pH is also highlighted in Figure 6. The Δi reached the maximum at pH 7.4. In order to achieve maximum sensitivity, the phosphate buffer solution of pH 7.4 was chosen as the most suitable medium in subsequent experiments.

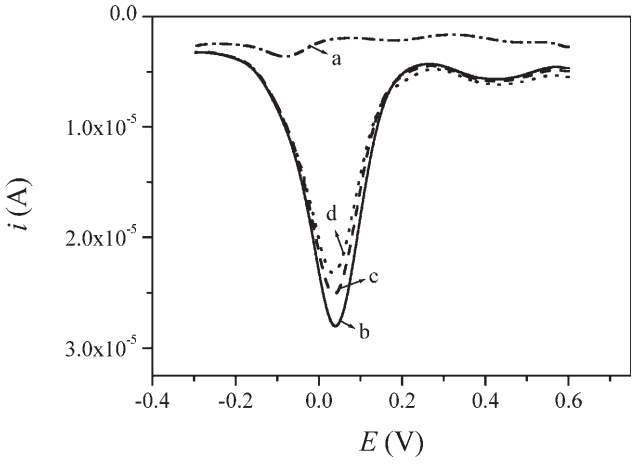

Fig. 4. Square-wave voltammograms at Au/MA/PAMAM/nano-Au/Tyr electrode. Scan rat: 100 mV s^{-1}. 0.1 mol L^{-1} PBS (pH 7.0) $+1.25 \times 10^{-4}$ mol L^{-1} PCA (a); 0.1 mol L^{-1} PBS (pH 7.0) $+2.0 \times 10^{-4}$ mol L^{-1} catechol (b); 0.1 mol L^{-1} PBS (pH 7.0) $+2.0 \times 10^{-4}$ mol L^{-1} catechol $+1.25 \times 10^{-5}$ mol L^{-1} PCA (c); 0.1 mol L^{-1} PBS (pH 7.0) $+2.0 \times 10^{-4}$ mol L^{-1} catechol $+$ 2.5×10^{-5} mol L^{-1} PCA (d).

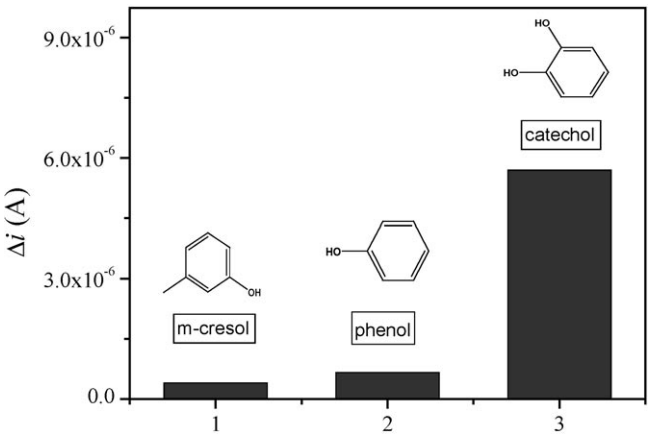

Fig. 5. Electrochemical detection of PCA using tyrosinase biosensor with different redox cosubstrates. Concentration of redox cosubstrates: 2.0×10^{-4} mol L^{-1}; concentration of PCA: 2.5×10^{-5} mol L^{-1} and concentration of PBS (pH 7.4): 0.1 mol L^{-1}.

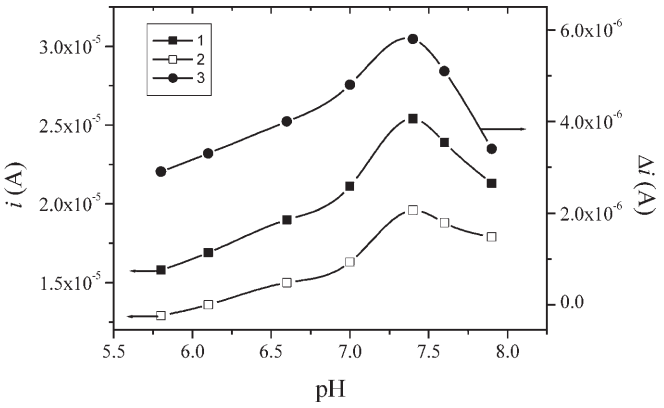

Fig. 6. Effect of pH on the peak currents. 1) i for 2.0×10^{-4} mol L^{-1} catechol; 2) i for 2.0×10^{-4} mol L^{-1} catechol $+ 2.5 \times 10^{-5}$ mol L^{-1} PCA; 3) Δi for 2.0×10^{-4} mol L^{-1} catechol $+ 2.5 \times 10^{-5}$ mol L^{-1} PCA. Concentration of PBS, 0.1 mol L^{-1}.

3.5. Effect of Concentration of Catechol

The effect of concentration of catechol on the enzyme electrode response was investigated by varying the concentration of catechol from 2.0×10^{-5} to 6.0×10^{-4} mol L^{-1} and the results are displayed in Figure 7. The peak currents of catechol and catechol-PCA system increase with the concentration of catechol increase. However, the Δi distinctly enhances and almost becomes constant, when the concentration of catechol is above 2.0×10^{-4} mol L^{-1}.

3.6. Quantitative Detection of PCA

Under the optimum conditions given above, quantitative detection of PCA at the tyrosinase modified electrode was investigated. Figure 8 shows square-wave voltammograms for different PCA concentrations. The dependence of the change of peak current on the concentration of PCA was

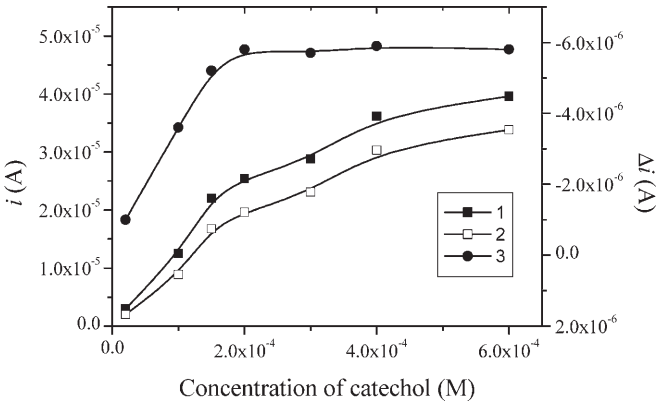

Fig. 7. Effect of concentration of catechol on the peak currents. 1) i for different concentration of catechol; 2) i for different concentration of catechol $+ 2.5 \times 10^{-5}$ mol L^{-1} PCA; 3) Δi for different concentration of catechol $+ 2.5 \times 10^{-5}$ mol L^{-1} PCA. Concentration of PBS, 0.1 mol L^{-1} (pH 7.4).

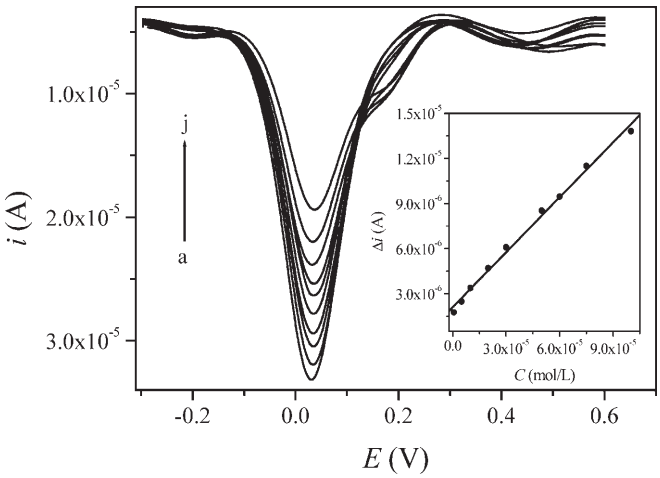

Fig. 8. Square-wave voltammograms of PCA at Tyr/nano-Au/PAMAM/MA electrode. Concentration of catechol: 2.0×10^{-4} mol L^{-1}; concentration of PCA from a) to j) are 0.0, 7.5×10^{-7}, 5.0×10^{-6}, 1.0×10^{-5}, 2.0×10^{-5}, 3.0×10^{-5}, 5.0×10^{-5}, 6.0×10^{-5}, 7.5×10^{-5}, and 1.0×10^{-4} mol L^{-1}, respectively; concentration of PBS (pH 7.4): 0.1 mol L^{-1}.

linear in the range of 7.5×10^{-7} to 1.0×10^{-4} mol l^{-1}. The linear response equation for the Δi and PCA concentration (C) was as follows:

$$\Delta i \text{ (A)} = 2.10 \times 10^{-6} + 0.122\, C \text{ (mol L}^{-1}\text{)},$$

and the correlation coefficient was 0.997. The detection limit ($S/N = 3$) was 5.4×10^{-8} mol L^{-1}.

3.7. Reproducibility and Stability

The reproducibility of the tyrosinase-modified electrode was studied by detection of 2.5×10^{-5} mol L^{-1} PCA solution at the optimum conditions. The relative standard deviation (RSD) was 3.6% for eight successive measurements. The electrode-to-electrode reproducibility was determined from the response to 2.5×10^{-5} mol L^{-1} PCA at four different enzyme electrodes that were prepared under the same conditions, an acceptable reproducibility was obtained with a variation coefficient of 4.8%. The sensor's storage stability was examined. The results showed that the activity of the biosensor reduced gradually. The enzyme electrode was stored in PBS at 4 °C. It retained 86% of the initial current response after seven days.

3.8. Interference Study

Excipients frequently added to dosage forms are talc, starch, titanium oxide, poly(ethylene glycol), magnesium stearate and lactose. Since talc, starch, titanium dioxide, poly(ethylene glycol) and magnesium stearate do not dissolve in 0.1 mol L^{-1} phosphate buffer, they were filtered out in the sample preparation step. Therefore, they did not interfere

Table 2. Determination of PCA in tablets of PCA.

No.	Specified [a] (mg/tablet)	Found ($n=5$) (mg/tablet)	*RSD* (%)
1	250.00	248.82	4.0
2	250.00	251.13	3.3
3	250.00	248.97	3.8

[a] From Shanghai Pharmaceutical Co. Ltd..

Table 3. Assays for recovery of the determination of PCA.

No.	Specified [a] (10^{-6} mol L^{-1})	Added (10^{-6} mol L^{-1})	Found ($n=5$) (10^{-6} mol L^{-1})	*RSD* (%)	Recovery (%)
1	3.35	2.00	5.29	4.2	97.0
2	3.35	4.00	7.51	3.5	104.0
3	6.70	2.00	8.80	2.9	105.0
4	6.70	4.00	10.62	3.7	98.0

[a] From Shanghai Pharmaceutical Co. Ltd.

with the determination of PCA. Lactose and poly(ethylene glycol) can dissolve in 0.1 mol L^{-1} phosphate buffer, so their influence on the determination of 2.5×10^{-5} mol L^{-1} PCA was investigated. It was found the tolerance limit for the ratio between PCA and lactose concentrations was 640. This caused an error of not more than $\pm 5\%$. Poly(ethylene glycol) almost did not interfere the determination of PCA and the tolerance limit for the ratio between PCA and poly(ethylene glycol) concentration at least was 2000.

3.9. Analytical Applications

The samples of tablets of PCA were determined after preparation. For each analysis, a tablet was powered in a mortar and dissolved with doubly distilled water, and the solution was displaced to a 100 mL volumetric flask and diluted to the mark with water. The solution was filtered for analysis. Different samples were determined and the determination results are shown in Table 2. There was no significant difference between the labeled contents and those obtained by the proposed method. Different standard concentrations of PCA were added to the real samples, and the determination results are listed in Table 3. These results indicated that the proposed method has good precision, and can be applied to the determination of PCA in pharmaceutical and biological fields.

4. Conclusions

A novel strategy based on immobilization of tyrosinase to a nano-Au monolayer, which was supported by amino groups of G4 PAMAM dendrimer monolayer and the PAMAM dendrimer membrane was successfully anchored on the MA-modified gold electrode through EDC cross-linking has been put forward. According to the facts that tyrosinase can catalyze the oxidation of *o*-diphenols to *o*-quinones and PCA can react with *o*-quinone through the Michael type addition, a new biosensor for determination of PCA was developed. The prepared biosensor exhibited a good performance in terms of sensitivity, operational stability and nice reproducibility.

5. Acknowledgements

This work was supported by the Korea Science and Engineering Foundation (KOSEF) grant funded by the Korea government (MOST) through the Bioelectronics Program (M10536000001 – 06N3600-00110), the Basic Research Program (R01-2005-000-10503-0), and the National R&D Project for Nano Science and Technology.

6. References

[1] D. T. Felson, J. J. Anderson, R. F. Meenan, *Arth. Rheum.* **1990**, *33*, 1449.
[2] J. S. Jones, *Thorax* **1987**, *42*, 988.
[3] H. A. Kim, Y. W. Song, *Rheumatol. Int.* **1997**, *17*, 5.
[4] F. E. O. Suliman, H. A. J. Al-Lawati, A. M. Z. Al-Kindy, I. E. M. Nour, S. B. Salama, *Talanta* **2003**, *61*, 221.
[5] B. P. Issopoulos, S. E. Salta, *IL Farmaco* **1997**, *52*, 113.
[6] A. A. Al-Majed, *J. Pharm. Biomed. Anal.* **1996**, *21*, 827.
[7] B. Gómez-Taylor Corominas, J. Pferzschner, M. Catalá Icardo, L. Lahuerta Zamora, J. Martínez Calatayud, *J. Pharm. Biomed. Anal.* **2005**, *39*, 281.
[8] A. A. Al-Majed, *Anal. Chim. Acta* **2000**, *408*, 169.
[9] T. P. Ruiz, C. Martinez-Lozano, V. Tomas, C. S. de Cardona, *J. Pharm. Biomed. Anal.* **1996**, *15*, 33.
[10] Z. D. Zhang, W. R. G. Baeyens, X. R. Zhang, G. Van Der Weken, *Analyst*, **1996**, *121*, 1569.
[11] Z. Zhang, W. R. G. Baeyens, X. Zhano, G. V. D. Weken, *Anal. Chim. Acta* **1997**, *347*, 325.
[12] N. Radic, J. Komljenovic, D. Dobcnik, *Croat. Chem. Acta* **2000**, *73*, 263.
[13] R. F. Bergstrom, D. R. Kay, J. G. Wagner, *J. Chromatogr. B* **1981**, *222*, 445.

[14] F. Nachtmann, *Int. J. Pharm.* **1980**, *4*, 337.
[15] J. Russell, J. A. McKeown, C. Hensman, W. E. Smith, J. Reglinski, *J. Pharm. Biomed. Anal.* **1997**, *15*, 1757.
[16] M. Wronski, *J. Chromatogr. B* **1996**, *676*, 29.
[17] A. Zinellu, C. Carru, S. Sotgia, L. Deiana, *J. Chromatogr. B* **2004**, *803*, 299.
[18] J. Nelson, *J. Assoc. Offic. Anal. Chem.* **1981**, *64*, 1174.
[19] S. Shahrokhian, A. Souri, H. Khajehsharifi, *J. Electroanal. Chem.* **2004**, *565*, 95.
[20] N. Wangfuengkanagul, O. Chailapakul, *Talanta* **2002**, *58*, 1213.
[21] A. A. J. Torriero, E. Salinas, E. J. Marchevsky, J. Raba, J. J. Silber, *Anal. Chim. Acta* **2006**, *580*, 136.
[22] S. Shahrokhian, S. Bozorgzadeh, *Electrochim. Acta* **2006**, *51*, 4271.
[23] D. A. Tomalia, *Prog. Polym. Sci.* **2005**, *30*, 294.
[24] L. Sun, R. M. Crooks, *J. Phys. Chem. B* **2002**, *106*, 5864.
[25] D. Cakara, J. Kleimann, M. Borkovec, *Macromolecules* **2003**, *36*, 4201.
[26] E. Kim, K. Kim, H. Yang, Y. T. Kim, J. Kwak, *Anal. Chem.* **2003**, *75*, 5665.
[27] J. Ledesma-Garcia, J. Manriquez, S. Gutierrez-Granados, L. A. Godinez, *Electroanalysis* **2003**, *15*, 659.
[28] S. J. Kwon, E. Kim, H. Yang, J. Kwak, *Analyst* **2006**, *131*, 402.
[29] S. Q. Liu, D. Leech, H. X. Ju, *Anal. Lett.* **2003**, *36*, 1.
[30] E. Katz, I. Willner, J. Wang, *Electroanalysis* **2004**, *16*, 19.
[31] D. Chen, G. Wang, J. H. Li, *J. Phys. Chem. C* **2007**, *111*, 2351.
[32] S. Seo, V. K. Sharma, N. Sharma, *J. Agric. Food Chem.* **2003**, *51*, 2837.
[33] I. Willner, M. Lion-Dagan, S. Marx-Tibbon, E. Katz, *J. Am. Chem. Soc.* **1995**, *117*, 6581.
[34] J. Manriquez, E. Juaristi, O. Munoz-Muniz, L. A. Godinez, *Langmuir* **2003**, *19*, 7315.
[35] L. Alfonta, I. Willner, D. J. Throckmorton, A. K. Singh, *Anal Chem.* **2001**, *73*, 5287.
[36] F. Sundfors, J. Bobacka, A. Ivaska, A. Lewenstam, *Electrochim. Acta* **2002**, *47*, 2245.
[37] I. Szymańska, H. Radecka, J. Radecki, R. Kaliszan, *Biosens. Bioelectron.* **2007,** *22*, 1955.
[38] M. Friedman, *J. Agric. Food Chem.* **1994**, *42*, 3.
[39] J. J. L. Cilliers, V. L. Singleton, *J. Agric. Food Chem.* **1990**, *38*, 1789.

